Journal of Molecular and Cellular Cardiology 96 (2016) 26–37

Contents lists available at ScienceDirect

Journal of Molecular and Cellular Cardiology

journal homepage: www.elsevier.com/locate/yjmcc

Nuclear proton dynamics and interactions with calcium signaling

Alzbeta Hulikova, Pawel Swietach *

Burdon Sanderson Cardiac Science Centre, Department of Physiology, Anatomy and Genetics, Parks Road, Oxford OX1 3PT, United Kingdom

ARTICLE INFO

Article history:
Received 24 April 2015
Received in revised form 2 June 2015
Accepted 7 July 2015
Available online 13 July 2015

Keywords:
Protons
Nucleus
Cardiac myocyte
Calcium
Mobile buffer

ABSTRACT

Biochemical signals acting on the nucleus can regulate gene expression. Despite the inherent affinity of nucleic acids and nuclear proteins (*e.g.* transcription factors) for protons, little is known about the mechanisms that regulate nuclear pH (pH_{nuc}), and how these could be exploited to control gene expression. Here, we show that pH_{nuc} dynamics can be imaged using the DNA-binding dye Hoechst 33342. Nuclear pores allow the passage of medium-sized molecules (calcein), but protons must first bind to mobile buffers in order to gain access to the nucleoplasm. Fixed buffering residing in the nucleus of permeabilized cells was estimated to be very weak on the basis of the large amplitude of pH_{nuc} transients evoked by photolytic H^+-uncaging or exposure to weak acids/bases. Consequently, the majority of nuclear pH buffering is sourced from the cytoplasm in the form of mobile buffers. Effective proton diffusion was faster in nucleoplasm than in cytoplasm, in agreement with the higher mobile-to-fixed buffering ratio in the nucleus. Cardiac myocyte pH_{nuc} changed in response to maneuvers that alter nuclear Ca^{2+} signals. Blocking Ca^{2+} release from inositol-1,4,5-trisphosphate receptors stably alkalinized the nucleus. This Ca^{2+}-pH interaction may arise from competitive binding to common chemical moieties. Competitive binding to mobile buffers may couple the efflux of Ca^{2+} *via* nuclear pores with a counterflux of protons. This would generate a stable pH gradient between cytoplasm and nucleus that is sensitive to the state of nuclear Ca^{2+} signaling. The unusual behavior of protons in the nucleus provides new mechanisms for regulating cardiac nuclear biology.

1. Introduction

A vast majority of biologically important molecules react reversibly with protons (H^+ ions) [1]. This chemical interaction underlies the pH-sensitivity observed with essentially all biological processes, including those that underlie cardiac function. The complex effects of protons on metabolism, electrical excitation, calcium signaling and contraction have been investigated experimentally [1] and modeled mathematically [2]. However, comparatively little is known about the effect of pH on nuclear biology. This is despite the inherent affinity of nucleic acids and nuclear proteins for protons, and hence a predicted pH-sensitivity. In particular, pH is likely to influence the activity of transcription factors such as EGR1 (Early-Growth Response 1), ERα (Estrogen Receptor α), GCR (Glucocorticoid receptor) and NFκB (Nuclear Factor kappa-light-chain-enhancer of activated B-cells) which contain protonatable histidine residues near sites of interaction with DNA [3–6]. Of relevance to the heart, the DNA-binding motif of NFAT (Nuclear Factor of Activated T-cells), a transcription factor involved in pro-hypertrophic signaling [7,8], contains conserved histidines residues.

Protons can affect cardiac function indirectly by modulating the dynamics of other signaling molecules, such as Ca^{2+} ions [9–11]. Nuclear activity in cardiac myocytes is strongly regulated by Ca^{2+} signals evoked by chemical messengers, notably inositol 1,4,5-trisphosphate ($InsP_3$) [12–14]. The molecular apparatus regulating transcription must distinguish $InsP_3$-evoked Ca^{2+} signals from electrically-evoked Ca^{2+} transients that flood the cell. Pro-hypertrophic nuclear Ca^{2+} signals are believed to operate within highly localized microdomains that are insulated from $[Ca^{2+}]$ fluctuations associated with excitation–contraction coupling [15]. It is well-documented that pH strongly modulates Ca^{2+} signaling in the cytoplasm [1,9,16]. Moreover, a gradient of pH can compartmentalize cytoplasmic $[Ca^{2+}]$ by means of a recently described Ca^{2+}/H^+ exchange process that operates without membranes [9]. This process could, in principle, generate stable $[Ca^{2+}]$ gradients between the nucleus and cytoplasm. However, evidence for Ca^{2+}/H^+ interactions in the nucleus is lacking, therefore the role of pH_{nuc} in regulating Ca^{2+}-sensitive gene expression is unknown.

The physiological and pathophysiological significance of pH-sensitivity must be evaluated in the context of proton dynamics, that is, the reactive, diffusive and transport fluxes that set pH. In the heart, proton fluxes can reach several mmol/l/min, which is very large in comparison with steady-state intracellular $[H^+]$ (normally in the sub-μM range). High cytoplasmic pH-buffering, distributed among the cell's titratable chemical moieties, restricts proton diffusivity [17,18] and attenuates the amplitude and rate of pH changes evoked by fluxes such as metabolic acid production or membrane transport of acid [19,20]. In contrast to the wealth of information about proton behavior in cytoplasm, little is known about proton dynamics in the nucleus. Moreover,

* Corresponding author.
E-mail address: pawel.swietach@dpag.ox.ac.uk (P. Swietach).

http://dx.doi.org/10.1016/j.yjmcc.2015.07.003

it is often assumed [21] that pH_{nuc} is tightly coupled to cytoplasmic pH (pH_{cyto}) by means of high-conductance nuclear pores, thus precluding the manifestation of nucleus-specific behavior.

Here, we investigate proton dynamics in the nucleus and compare these with proton behavior in cytoplasm. Our data show that, despite the presence of nuclear pores, protons cannot freely enter the nucleus but require mobile buffers to facilitate the transfer. We also demonstrate that buffering by fixed sites residing in the nucleus is surprisingly weak. As a result, effective proton diffusivity in the nucleus is faster than in cytoplasm. Since proton transmission in and out of the nucleus is mediated by mobile buffers, a gradient of pH could be established between the nucleus and cytoplasm ($\Delta pH = pH_{nuc} - pH_{cyto}$) by directing the flow of protonated mobile buffer molecules. Indeed, maneuvers that alter nuclear Ca^{2+} signaling can stably change ΔpH, and we hypothesize that this may involve the exchange of Ca^{2+}-bound mobile buffers for their protonated form [9]. The unusual dynamics of protons in the nucleus, and interactions with calcium provide new means of interacting with the gene expression.

2. Materials and methods

2.1. Cells

Adult ventricular myocytes were isolated enzymically from Langendorff-perfused Sprague–Dawley rat hearts and kept in DMEM suspension for up to 8 h. Neonatal cardiac ventricular myocytes were isolated enzymically from rat pups and cultured for 48 h in LabTek chambers. Animals were sacrificed in accordance with Home Office regulations on Schedule I killing. NHDF-Ad human dermal fibroblasts (acquired from Lonza, Slough, UK) and colorectal HCT116 cancer cells (acquired from ATCC, Teddington, UK) were cultured until confluent in LabTek chambers.

2.2. Superfusion and solutions

Adult cardiac myocytes were superfused at 37 °C in a custom-made Perspex chamber with a poly-L-lysine treated coverslip at its base. Superfusion of neonatal cardiac myocytes, NHDF-Ad fibroblasts or HCT116 cells was performed in LabTek chambers used for culturing. Superfusion chambers were mounted on a Zeiss Axiovert inverted microscope coupled to an LSM 700 confocal imaging system. Two platinum electrodes attached to the Perspex chamber delivered field stimulation for pacing adult myocytes. CO_2/HCO_3^- buffered Tyrode was bubbled with 5% CO_2 and contained 125 mM NaCl, 4.5 mM KCl, 11 mM glucose, 22 mM $NaHCO_3$, 1 mM $CaCl_2$, 1 mM $MgCl_2$. For Hepes-buffered Tyrode, 22 mM HCO_3^- was replaced with 20 mM Hepes, NaCl was raised to 135 mM and solution was titrated to pH 7.4 with 4 M NaOH. 0Na0Ca solution contained 135 mM N-methyl-D-glucamine, 4.5 mM KCl, 11 mM glucose, 20 mM Hepes, 0.5 mM EGTA, 1 mM $MgCl_2$, titrated to pH 7.4 with 5 M HCl. High-Hepes internal solution (IS) contained 30 mM KCl, 90 mM K-gluconate, 10 mM NaCl, 20 mM Hepes, 2 mM MgATP, 0.1 mM ADP, 1 mM BAPTA, 0.5 mM $MgCl_2$, 0.6 mM $CaCl_2$, pH titrated to 7.0–7.1 with KOH (final free $[Ca^{2+}] = 0.1$ μM, $[Mg^{2+}] = 0.5$ mM). For alkaline IS, pH was titrated to 7.5. For acidic IS, pH was titrated to 6.6 or 6.5, and $CaCl_2$ and $MgCl_2$ were reduced appropriately (final free $[Ca^{2+}] = 0.1$ μM, $[Mg^{2+}] = 0.5$ mM). The concentrations of divalents added to solutions was determined from ionic equilibria using CaBuf program (G. Droogmans, ftp://ftp.cc.kuleuven.ac.be/pub/). Low-Hepes IS contained only 0.5 mM Hepes and an additional 15 mM of K-gluconate; for experiments on permeabilized adult myocytes, MgATP was raised to 3 mM to reduce the extent of rigor. For acetate or ammonium containing IS, KCl was iso-osmotically replaced with NH_4Cl or K-Acetate. Permeabilization was performed in high-Hepes IS containing 0.005% saponin. For photolytic uncaging of acid, solutions contained 6-nitroveratraldehyde (Sigma-Aldrich, UK), a photolabile H^+-donor excited at 405 nm (dissolved in warm solution from stock in DMSO).

2.3. Fluorescence imaging

A Zeiss LSM 700 confocal imaging system recorded fluorescence in superfused cells. The Ca^{2+} reporter dye Fluo3 (20 μM; loaded into cells as the AM-ester for 5 min at room temperature) was excited at 488 nm and emission was recorded >520 nm. Fluo3 was calibrated by measuring the fluorescence response to 100 μM Ca^{2+} dialyzed into cells *via* patch pipette (this measures the maximal fluorescence, F_{max}). This experiment estimates Fluo3 Ca^{2+} affinity *in situ*, assuming that Ca^{2+}-independent fluorescence (F_{min}) is zero and that resting $[Ca^{2+}]$ is 100 nM [9]. The pH-sensitive fluorescence dye cSNARF1 (10 μM; loaded into cells as the AM-ester for 10 min at room temperature) was excited at 555 nm and emission was recorded ratiometrically at 580 ± 20 nm and 640 ± 20 nm. The nuclear dye Hoechst 33342 (loaded at 1:1000 dilution for 30 min at room temperature) was excited at 405 nm and emission was recorded ratiometrically (shortpass filter <470 nm and bandpass filter 490–555 nm). All dyes were obtained from Life Technologies (UK). Higher intensity 405 nm laser was used to release acid from the caged H^+-compound 6-nitroveratraldehyde.

3. Results

3.1. Cytoplasmic proton dynamics are attenuated by high buffering capacity

During the cardiac cycle, electrical excitation evokes large Ca^{2+} fluxes across the sarcolemmal and sarcoplasmic reticulum membranes that raise cytoplasmic $[Ca^{2+}]$ transiently. Fig. 1A shows the averaged time course of a Ca^{2+} transient recorded in linescan mode (3 ms/scan) in a Fluo3-loaded adult ventricular myocyte paced at 1 Hz. Ca^{2+} activates the contractile apparatus, which consumes ATP. Estimates of the turnover of intracellular ATP are ~10 s (resting heart) to ~2 s (maximally-activated heart) [22], predicting that a significant fraction of the myocytes' ATP pool (several mM) is hydrolyzed during the relatively short period of tension development. Since ATP hydrolysis is a net proton-generating reaction (0.5–1.0 H^+/ATP stoichiometry over the pH_{cyto} range 6.5–7.5) [23], a concentrated release of protons is expected to take place during contraction. To explore whether force generation is associated with a measurable 'proton transient', cSNARF1-loaded adult rat ventricular myocytes (superfused with 5% CO_2/22 mM HCO_3^- Tyrode at 37 °C) were field-stimulated at 1 Hz (1 ms pulse) and fluorescence was measured in linescan mode (1.9 ms/scan) along the long-axis of the cell, avoiding nuclear regions. The width of the fluorescence signal along the linescan was used as an index of contraction (Fig. 1B gray trace, inverted for comparison with $[H^+]$ time course). Contraction was accompanied by a proton transient of ~3.6 nM (95.3 ± 0.0002 nM to 99.0 ± 0.01 nM). Since cSNARF1 fluorescence was acquired ratiometrically, the pH response is unlikely to be an artifact of cell movement. This assertion is supported by the short delay between changes in cell-length and $[H^+]$. The proton transient was abolished by treatment with the contraction inhibitor butanedione monoxime (10 mM; data not shown), suggesting that the pH response was not due to electrical activity

or Ca^{2+} signaling *per se*. The small size of the proton transient, despite the expected release of ~mM of protons per contraction, is a consequence of high buffering capacity. Total buffering capacity (β) in myocyte cytoplasm at resting pH is ~50 mM/pH, equivalent to a dimensionless buffering ratio (B) of 200,000:1

$$\frac{d[H^+]_{total}}{d[H^+]_{free}} = \frac{[H^+]_{total}}{d\mathrm{pH}} \times \frac{d\mathrm{pH}}{d[H^+]_{free}}, \therefore B = \frac{\beta}{\log(10) \times [H^+]}.$$

Assuming that buffering kinetics are fast, a 3.6 nM proton transient is thus predicted to arise from a ~0.7 mM release of H^+ ions, *i.e.* hydrolysis of a tenth of the ATP pool. In summary, high cytoplasmic buffering attenuates proton dynamics in contracting myocytes.

3.2. Imaging cytoplasmic and nuclear pH simultaneously

The pH-sensitivity of the nuclear stain Hoechst 33342 was exploited to study nuclear pH dynamics [24]. Acidity increases total fluorescence emission and produces a spectral shift that permits ratiometric measurements. An optimal combination of wide dynamic range and good signal-to-noise ratio is obtained by sampling 405 nm-excited fluorescence at ~440 nm (470 nm shortpass filter) and ~510 nm (490–555 bandpass filter). Since the spectra of cSNARF1 and Hoechst 33342 do not overlap, both dyes can be used concurrently to probe cytoplasmic and nuclear pH by alternating between 555 nm and 405 nm excitation, respectively (Fig. 2A). Artifactual signal bleed-through between cSNARF1 and Hoechst 33342 detection modes was tested in myocytes loaded with one dye only at a time. In cSNARF1 detection mode, fluorescence from Hoechst 33342 was essentially absent (the nuclear dye is not excited at 555 nm). In Hoechst 33342 detection mode, fluorescence from cSNARF1 was very low compared to the signal from Hoechst 33342 (Fig. 2B). Since both dyes can be loaded into cells passively, experiments can be performed on freshly isolated myocytes without genetic modifications. Using image analysis of confocally-acquired data to identify nuclear regions, it is possible to measure pH_{nuc} and the surrounding pH_{cyto}. Hoechst 33342 and cSNARF1 fluorescence ratios were calibrated using the nigericin technique [25]. Briefly, cells were superfused in solutions containing 140 mM KCl, 1 mM $MgCl_2$, 1 mM EGTA, 10 mM MES, 10 mM HEPES and 10 μM nigericin (a K^+/H^+ ionophore). To generate a pH-calibration curve for the co-loaded fluorescent dyes, intracellular pH was manipulated by changing superfusate pH (Fig. 2C). These data demonstrate an apparent pK_a and dynamic range (R_{max}/R_{min}) of 6.54 and 2.55, respectively, for Hoechst 33342 (c.f. 6.98 and 12.2 for cSNARF1). The Hoechst 33342 ratio did not change substantially during contraction, despite a 10-fold increase in $[Ca^{2+}]$ (Fig. 2D), arguing for its Ca^{2+}-insensitivity. Using the same procedure, the two dyes could be calibrated concurrently in neonatal ventricular myocytes, fibroblasts (NHDF-Ad) and colorectal epithelial cancer cells (HCT116).

3.3. Protons enter and exit the nucleus only when bound to mobile buffers

The pathway of least resistance to ion traffic between cytoplasm and nucleoplasm is the nuclear pore, known to conduct macromolecules as large as 100 kDa [21]. The diffusive restrictions imposed by the nucleus were explored by measuring the diffusion of calcein (a fluorescent marker of molecular weight 622 Da) following localized bleaching (FRAP: fluorescence recovery after photobleaching). Fig. 3A shows fluorescence recovery (excitation at 488 nm, fluorescence measured >510 nm) and the best-fit rate constant (the inverse of time constant). Experiments on adult myocytes were performed in 0Na0Ca superfusates to minimize motion artifacts. Bleaching was performed in one of two types of regions (see icons in Fig. 3B) in myocytes co-loaded with calcein-AM and Hoechst 33342. In the first set of experiments, the entire nucleus was selected for bleaching (region defined on the basis of Hoechst 33342 fluorescence). In the second set of experiments, bleaching was restricted to a 3 × 3 μm region in the nucleus. In both cases, bleaching was performed until half of the fluorescence signal was attenuated locally. FRAP experiments performed in nuclear regions were then repeated in regions of bulk cytoplasm using the same size and shape of the bleaching region. Calcein diffusivity in the nucleus was no different from

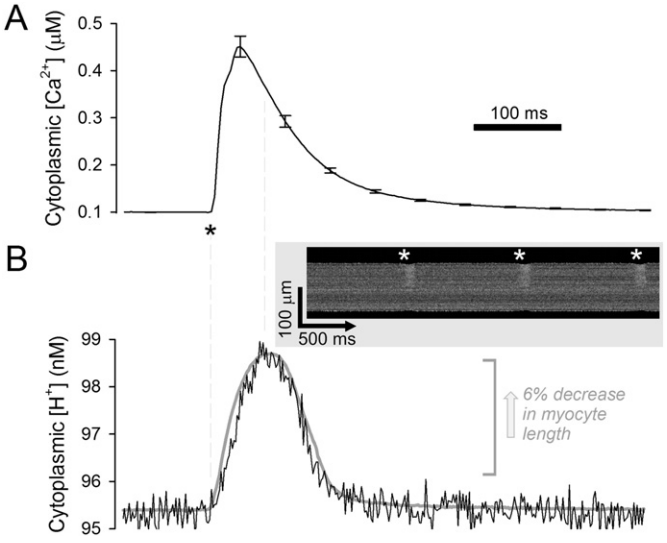

Fig. 1. Proton dynamics in the cytoplasm of contracting myocytes. (A) Adult ventricular myocytes loaded with Ca^{2+}-dye Fluo3. Electrical excitation (1 ms field stimulation at 1 Hz; *) evokes a Ca^{2+} transient (n = 10). (B) Adult ventricular myocytes, paced at 1 Hz, loaded with pH-dye cSNARF1. Electrical excitation triggers cell-shortening (gray line, inverted for comparison with $[H^+]$ time course). During contraction, cytoplasmic $[H^+]$ increases transiently ('proton transient'), putatively as a result of acid-yielding ATP hydrolysis by cross-bridge cycling (n = 17; SEMs not shown for clarity). Inset: linescan of cSNARF1 ratio.

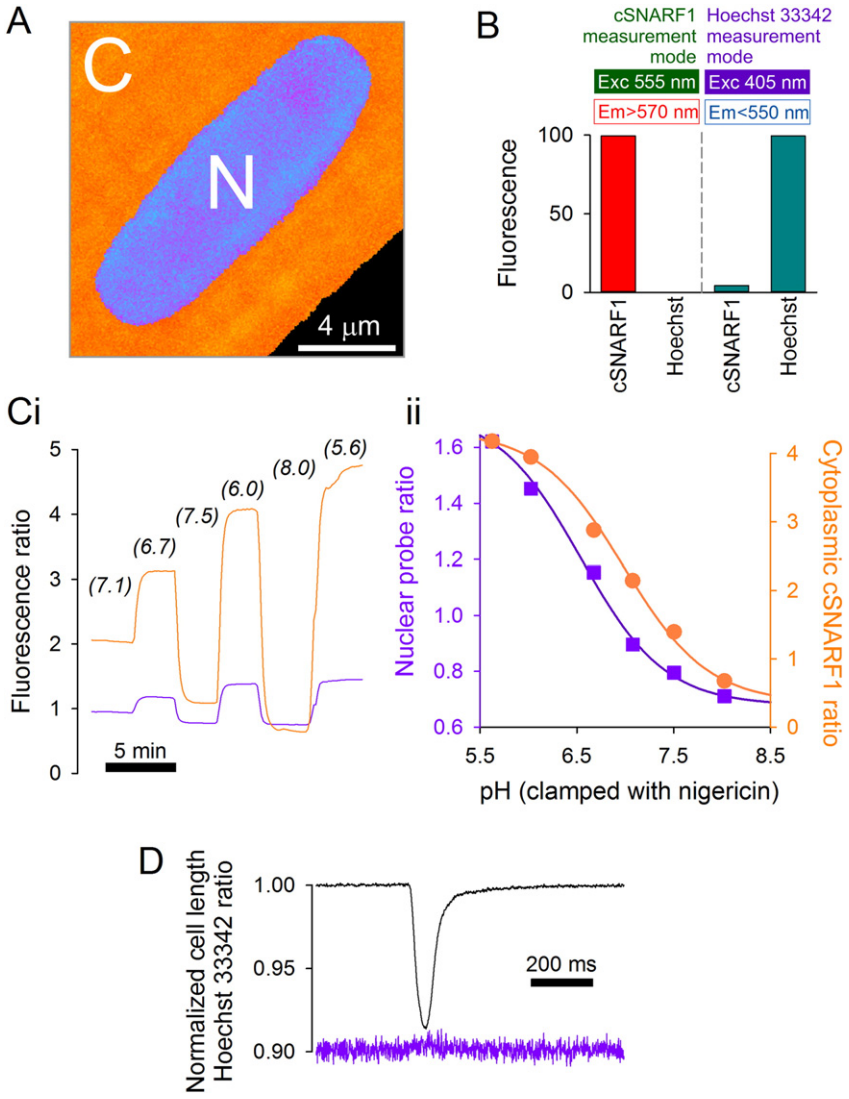

Fig. 2. Measuring nuclear and cytoplasmic pH simultaneously. (A) Adult ventricular myocyte loaded with cSNARF1 and DNA-binding Hoechst 33342 dyes. Perinuclear cSNARF1 reports cytoplasmic pH; Hoechst 33342 probes nuclear pH. (B) Absence of fluorescence bleed-through. In cSNARF1 detection mode (excitation at 555 nm; emission >570 nm), Hoechst 33342-loaded cells emit no fluorescence, compared to signal from cSNARF1-loaded cells. In Hoechst 33342 detection mode (excitation 405 nm; emission < 550 nm), cSNARF1-loaded cells emit considerably less (~20-fold) fluorescence than Hoechst 33342-loaded cells. (C) Simultaneous calibration of dyes in adult myocytes (n = 30) using nigericin (10 μM) protonophore. (i) Time course of intracellular cSNARF1 (orange) and Hoechst 33342 (purple) ratio during changes in extracellular pH in myocytes under superfusion. (ii) Calibration curve (Hoechst 33342 = squares; cSNARF1 = circles). (D) Hoechst 33342 ratio (purple) does not change in response to a rise in $[Ca^{2+}]$ evoked by electrical pacing.

that in the cytoplasm, even when Ca^{2+} stores were emptied by thapsigargin (10 μM; blocker of the smooth/endoplasmic reticulum Ca^{2+} ATPase, SERCA). Similarly, no difference in FRAP was measured between nuclear and cytoplasmic regions of neonatal ventricular myocytes (experiments in 0Na0Ca or in normal Tyrode). Thus, the sum of nucleoplasmic tortuosity and nuclear pore permeability restrict calcein diffusivity to the same extent as does the bulk cytoplasm. These results argue that nuclear pores are not major obstacles to the movement of medium-sized molecules, such as calcein.

Based on ionic radius alone, protons would be expected to flow in and out of the nucleus much faster than calcein. However, extensive buffering restricts the movement of free protons [26]. In cytoplasm, proton diffusion is facilitated by low-molecular weight (mobile) buffers, such as histidyl dipeptides [17,18]. Effective proton diffusivity (D_H^{eff}) is expressed mathematically as a function of free H^+ diffusivity (D_H), mobile buffer diffusivity (D_{mob}), and mobile and fixed buffering capacities (β_{mob}, β_{fix}):

$$D_H^{eff} = \frac{D_H \times \log(10) \times [H^+] + D_{mob} \times \beta_{mob}}{\log(10) \times [H^+] + \beta_{mob} + \beta_{fix}} \approx D_{mob} \times \frac{\beta_{mob}}{\beta_{mob} + \beta_{fix}}. \quad (1)$$

The role of mobile buffers in facilitating the exchange of protons between cytoplasm and nucleoplasm was explored in adult myocytes by measuring the rate of nuclear acidification in the presence and absence of intrinsic mobile buffers (Fig. 4A). In resting (not paced), intact adult ventricular myocytes (*i.e.* with all intrinsic mobile buffers retained), transient exposure to acetate-containing solution reversibly acidified the cytoplasm (cSNARF1) and nucleus (Hoechst 33342). The delay in pH response between the two compartments was very small, indicating good diffusive coupling (Fig. 4Ai). Experiments were repeated in saponin-permeabilized myocytes superfused with internal solution of low buffering power (0.5 mM

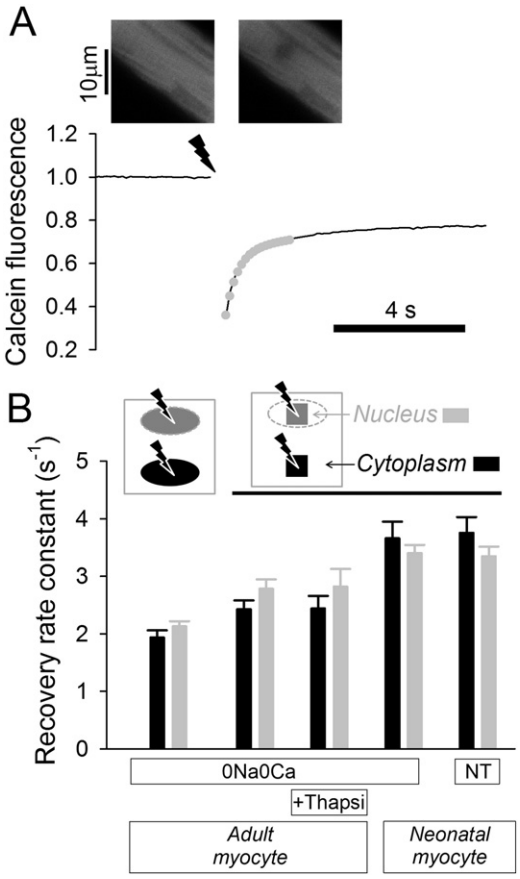

Fig. 3. Probing nuclear and cytoplasmic diffusive tortuosity. (A) Fluorescence recovery after photobleaching (FRAP) protocol for adult ventricular myocyte AM-loaded with calcein (the FRAP marker) and Hoechst 33342 (to identify nuclear regions). Superfusion with 0Na0Ca solution to block contraction. Bleaching in 3 × 3 μm region of cytoplasm evokes cytoplasmic calcein diffusion, quantified in terms of rate constant from exponential best-fit (gray dotted curve). (B). FRAP experiments performed on adult ventricular myocytes with bleaching regions set to the outline of nuclei or a 3 × 3 μm region within nuclei (identified by Hoechst 33342 fluorescence). FRAP repeated in bulk cytoplasm using the same bleaching configuration (n = 10–15 cells/histogram). Emptying sarcoplasmic reticulum Ca^{2+} stores with thapsigargin (Thapsi; 10 μM) did not affect calcein diffusivity. Experiments performed on neonatal ventricular myocytes in 0Na0Ca solution or normal Tyrode (NT) (n = 20–25 cells/histogram).

Hepes and 3 mM MgATP) to minimize mobile buffering capacity (NB: lower [Hepes] would lead to difficulties in titrating solutions to a stable pH; lower [ATP] may lead to movement artifacts due to hyper-contracture). Switching between superfusates at pH 7 and 6.6 evoked a delayed pH_{nuc} response reported by Hoechst 33342. To determine if this pH_{nuc} response was rate-limited by slow delivery and wash-out of acid in the extra-nuclear region, myocytes that had not been loaded with Hoechst 33342 were first saponin-permeabilized and then exposed for 30 s to a solution containing 10 μM of the pH-reporter fluorescein conjugated to wheat germ agglutinin (WGA). WGA-fluorescein binds to membrane-tethered proteins, thus staining the sarcolemma and nuclear envelope (Fig. 4Aii) [27]. The fluorescence signal in extra-nuclear regions reported a faster pH response than nuclear Hoechst 33342, indicating that proton access to the myocyte's nucleus across nuclear pores is the rate-limiting step that depends on mobile buffers availability.

The relationship between mobile buffering and proton transmission in and out of the nucleus was explored further in NHDF-Ad fibroblasts loaded with calcein (AM-ester) and Hoechst 33342. Compared to myocytes, fibroblasts have larger and more spherical nuclei for better resolution of pH_{nuc} dynamics. Furthermore, fibroblast nuclei are more readily accessible upon surface-membrane permeabilization across a thin layer of cytoplasm. To permeabilize the surface membrane only, 0.005% saponin solution was withdrawn at the onset of calcein fluorescence loss (Fig. 4B). The rate of calcein loss from the nucleus provided a measure of calcein permeability across nuclear pores. By varying the composition of internal solution, experiments were performed in the presence of high (20 mM) or very low (0.5 mM) concentrations of Hepes, an exogenous mobile buffer. Since ATP is also a mobile pH buffer, [MgATP] was restricted to 2 mM (buffering <1 mM/pH). Unlike cardiac myocytes, fibroblasts do not undergo a contractile response (rigor) at this low [ATP]. Proton flux in and out of the fibroblast nuclei was evoked by switching rapidly between superfusates titrated to 7.1 and 6.6 (Fig. 4B), and the pH_{nuc} response was reported by Hoechst 33342. Thus, each experiment measured a proton-to-calcein permeability ratio per nucleus. As shown in Fig. 4C, the permeability ratio was greater with higher [Hepes]. A plot of the permeability ratio against total mobile buffering capacity (Hepes plus MgATP; assuming pK_a of 7.31 and 6.49, respectively [9]) shows that mobile buffering is obligatory for proton transport in and out of the nucleus. This relationship also shows that protons enter (and exit) the nucleus more slowly than calcein if the mobile buffering capacity is below ~10 mM/pH (*nota bene*, equivalent to the intrinsic mobile buffering capacity of cardiac cytoplasm [17]). In summary, proton traffic in and out of the nucleus is relatively slow and must be carried aboard mobile buffers.

3.4. Proton buffering by fixed moieties resident in the nucleus is weak

Mobile buffers account for half of the total intrinsic buffering capacity in myocyte cytoplasm; the remainder being attributed to fixed buffers [18]. Fixed buffering capacity can be measured by disturbing pH_{nuc} in cells that have been permeabilized to remove intrinsic mobile buffers. Adult

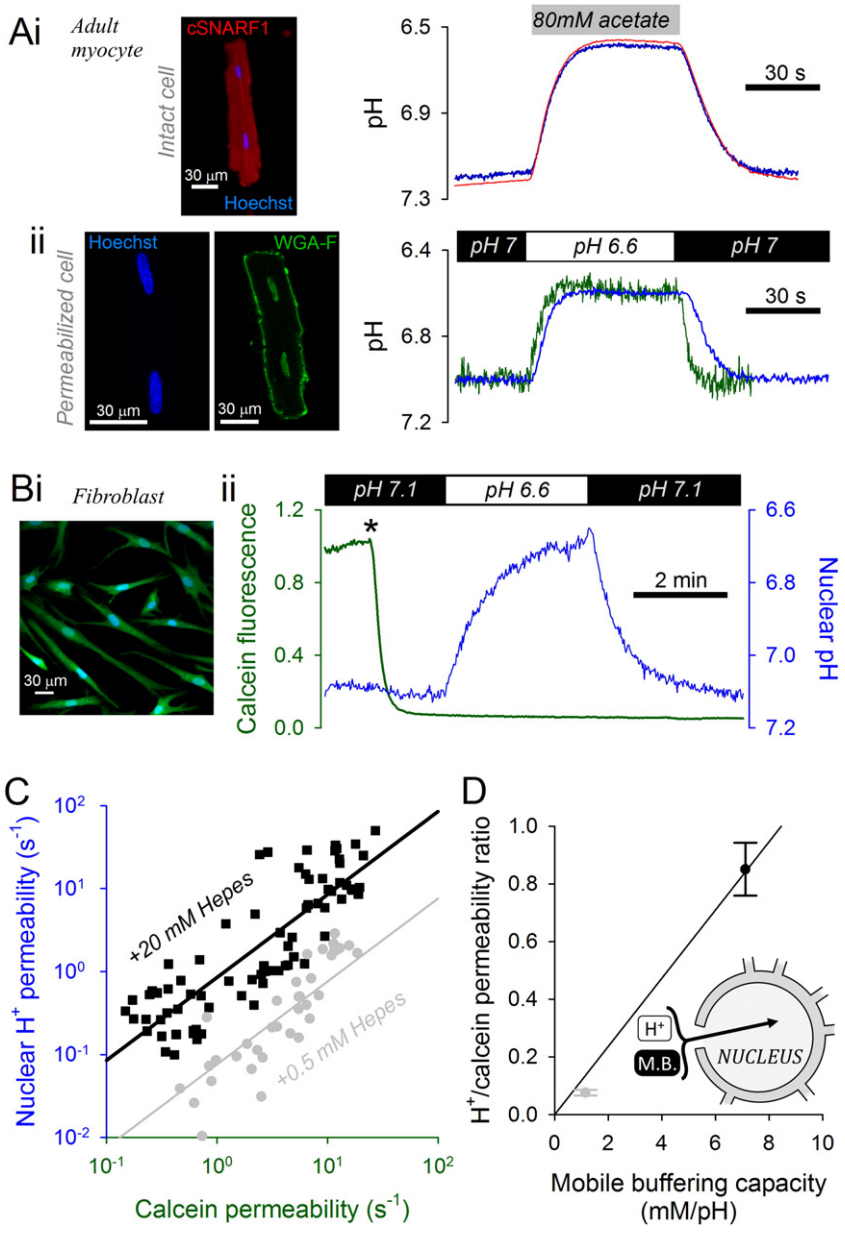

Fig. 4. Quantifying proton transmission into the nucleus. (A) (i) Intact adult ventricular myocyte (not paced electrically), loaded with cSNARF1 and Hoechst 33342. Transient exposure to 80 mM acetate evoked a rapid acidification in cytoplasm and, without delay, in the nucleus (average of 7 cells; SEMs <0.05 pH units; not shown for clarity). (ii) Permeabilized myocyte, superfused with low-buffer solution (0.5 mM Hepes, 3 mM ATP) loaded with Hoechst 33342 (to measure nuclear pH) or, in separate experiments, WGA-fluorescein (to measure extra-nuclear pH in nuclear-stained regions). Switching between superfusates at pH 7 and 6.6 evokes a rapid extra-nuclear pH response and a slower nuclear pH response (average of 8 cells; SEMs <0.03 for Hoechst 33342 and <0.06 for WGA-F; not shown for clarity). (B) (i) NHDF fibroblasts loaded with calcein and Hoechst 33342. (ii) Protocol for permeabilizing cells (0.005% saponin for <10 s at *) in internal solution buffered with 0.5 mM Hepes. Rate of nuclear calcein loss estimates calcein permeability. Transient exposure to acidic superfusate evokes proton traffic in and out of the nucleus, providing a read-out of proton permeability across nuclear pores. (C) Calcein permeability vs proton permeability with best-fit lines. Experiments performed using superfusates buffered with either 0.5 (n = 37) or 20 mM Hepes (n = 75). (D) Proton-to-calcein permeability ratio expressed as a function of total mobile buffering capacity supplied by superfusate (Hepes, $pK_a = 7.31$; MgATP, $pK_a = 6.49$). Inset: Proton transmission to the nucleus is facilitated by mobile buffers (M.B.).

myocytes, loaded with Hoechst 33342 were permeabilized and superfused with internal solution containing 0.5 mM Hepes and 3 mM ATP, to minimize mobile buffering, and 2 mM of 6-nitroveratraldehyde (NVA), a highly permeant photolabile H^+-donor. pH_{nuc} was reported by Hoechst 33342 under low intensity excitation to minimize background NVA photolysis. Higher intensity 405 nm excitation (raised ~100-fold relative to Hoechst excitation) was used to release protons from NVA in a controlled manner. A series of 5 exposures to high intensity 405 nm laser produced a large pH_{nuc} response (Fig. 5A; black trace). Assuming complete photolysis of NVA, the amplitude of this pH_{nuc} response suggests that nuclear pH buffering is very low (2 mM NVA evoking a 1.6 pH_{nuc} change is equivalent to a buffering capacity of 2/1.6 = 1.3 mM/pH). Of this, ~1 mM/pH buffering can be attributed to the presence of Hepes plus ATP. The relaxation time constant of the evoked pH_{nuc} transient was 8.0 ± 1.9 s, confirming a previous result (Fig. 4A) that the efflux of protons from the nucleus is slow in the absence of intrinsic mobile buffers. To demonstrate the effect of intrinsic mobile buffers on pH_{nuc} transients, experiments were repeated on intact myocytes loaded with Hoechst 33342 and superfused with 0Na0Ca solution. Uncaging protons using the same amount of energy as with permeabilized cells produced considerably smaller pH changes in nuclei that retain intrinsic mobile buffers (Fig. 5A; gray trace).

Fixed buffering capacity residing in the nucleus was measured using an alternative method. pH_{nuc} transients were evoked by exposing permeabilized cells to internal solution containing weak acids or bases. Hoechst 33342-loaded HCT116 cells were used for these experiments because their nuclei are larger (radius 5.8 ± 0.3 μm) and more spherical than those of the adult myocyte, while the cytoplasmic volume is very small. These conditions improve the power to resolve pH_{nuc} transients and minimize the distance from superfusate to the nucleus for more responsive pH_{nuc} manipulations. Upon saponin-permeabilization in 20 mM Hepes internal solution at pH 7.0, cells were transiently exposed to solution containing 40 mM ammonium/ammonia and then to solution containing 40 mM acetate/acetic acid at constant pH. These solution maneuvers did not alter pH_{nuc}, as expected from the high buffering capacity provided by Hepes (Fig. 5Bi). Experiments were repeated in solutions with very low (0.5 mM) [Hepes]. Exposure to ammonium/ammonia solution produced a transient decrease of pH_{nuc} of 0.29 units; whereas acetate/acetic acid solution evoked a 0.19-unit pH_{nuc} transient in the opposite direction (Fig. 5Bii). These responses suggest that in nucleoplasm, the charged species (ammonium, acetate) diffuse faster than the uncharged conjugate (ammonia, acetic acid). This behavior may be attributed to regions of nuclear hydrophobicity (low dielectric constant) [21,28], which may retard NH_3/acetic acid diffusion. On such a model, entry of ammonium (an acid) ahead of ammonia reduces pH_{nuc}, and entry of acetate (a base) ahead of acetic acid raises pH_{nuc} (Fig. 5Biii). The size of pH_{nuc} transients suggests that overall pH buffering is low. 40 mM NH_4^+ entering a compartment at pH 6.9 would, at equilibrium, produce 0.3 mM NH_3 and 0.3 mM H^+ ($=40 \times K_{NH4+}/([H^+] + K_{NH4+})$, $K_{NH4+} = 10^{-9.03}$ M). By analogy, 40 mM acetate would react with 0.16 mM H^+ to generate 0.16 mM acetic acid ($=40 \times [H^+]/([H^+] + K_{HAc})$,

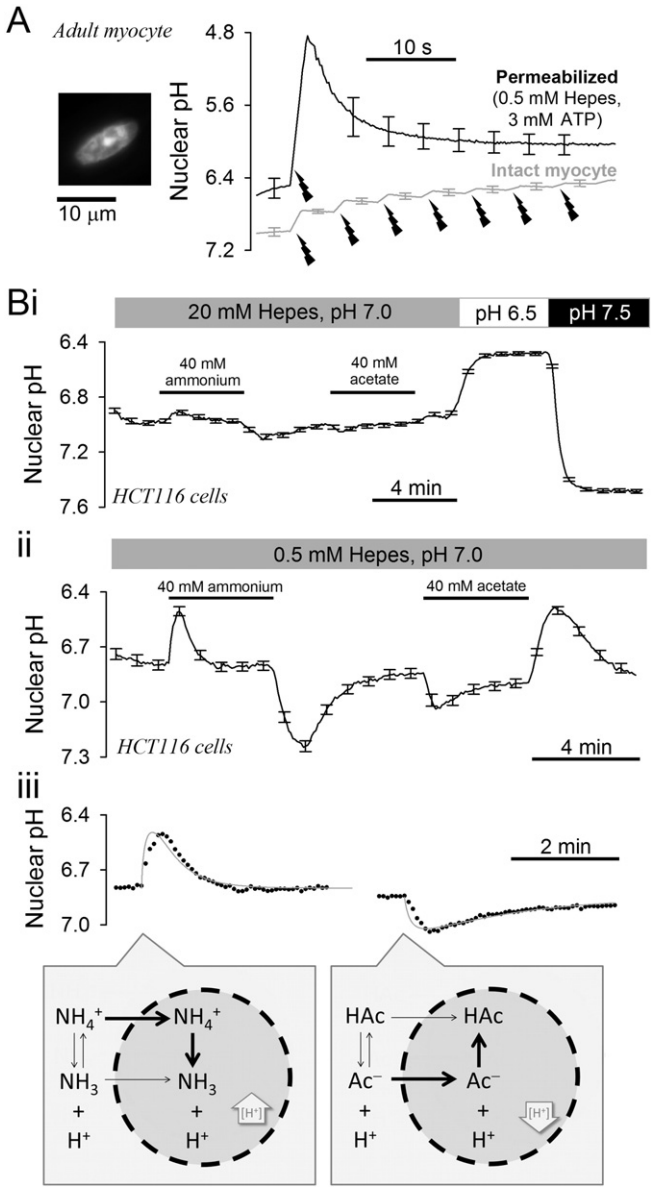

Fig. 5. Estimating fixed pH buffering capacity in the nucleus. (A) pH response in adult ventricular myocyte nucleus (Hoechst 33342-loaded) to photolytic uncaging of protons from 2 mM 6-nitroveratraldehyde in 16 × 16 μm region wholly containing the nucleus. In permeabilized cells superfused with low-buffer internal solution (0.5 mM Hepes, 3 mM ATP), the pH response is large and decays slowly (n = 6). Experiments repeated on intact cells (superfused with 0Na0Ca), demonstrating smaller pH responses to the same uncaging energy (n = 6). (B) Permeabilized, Hoechst 33342-loaded HCT116 cells. (i) Superfusion with internal solution containing 20 mM Hepes (n = 10). Exposure to 40 mM NH_4^+/NH_3 containing solution or 40 mM acetate/acetic acid containing solution at pH 7.0 did not alter nuclear pH. Calibration of Hoechst 33342 using superfusates titrated to pH 6.5 and 7.5 at end of experiment. (ii) Superfusion with 0.5 mM Hepes-buffered internal solution. Addition and removal of weak acid/weak base now evokes major changes in nuclear pH (n = 15). (iii) Model fits. Inset: scheme illustrating principle of nuclear pH transients.

$K_{HAc} = 10^{-4.5}$ M). Based on these estimates of acid uptake/release and the amplitude of pH_{nuc} transients, buffering capacity is estimated to be ~1 mM/pH. For a more accurate calculation that considers the slower entry of uncharged species, a model [29] was used for best fitting

$$\frac{dpH}{dt} = -\frac{(k_{on} \times K_{NH4+} \times [NH_4^+] - k_{on} \times [NH_3] \times [H^+]) + (k_{on} \times K_{HAc} \times [HAc] - k_{on} \times [Ac^-] \times [H^+])}{\beta_{fix}}$$

$$\frac{d[NH_3]}{dt} = D_{NH3} \times \left(\frac{d^2[NH_3]}{dr^2} + \frac{2}{r} \times \frac{d[NH_3]}{dr}\right) + (k_{on} \times K_{NH4+} \times [NH_4^+] - k_{on} \times [NH_3] \times [H^+])$$

$$\frac{d[NH_4^+]}{dt} = D_{NH4+} \times \left(\frac{d^2[NH_4^+]}{dr^2} + \frac{2}{r} \times \frac{d[NH_4^+]}{dr}\right) - (k_{on} \times K_{NH4+} \times [NH_4^+] - k_{on} \times [NH_3] \times [H^+])$$

$$\frac{d[Ac^-]}{dt} = D_{Ac} \times \frac{d^2[Ac^-]}{dr^2} + (k_{on} \times K_{HAc} \times [HAc] - k_{on} \times [Ac^-] \times [H^+])$$

$$\frac{d[HAc]}{dt} = D_{HAc} \times \frac{d^2[HAc]}{dr^2} - (k_{on} \times K_{HAc} \times [HAc] - k_{on} \times [Ac^-] \times [H^+]).$$

Here k_{on} is the protonation constant (10^{10} s^{-1}), K_{NH4+} and K_{HAc} are the ammonium and acetic acid dissociation constants ($10^{-9.03}$, $10^{-4.5}$ M), r is the radial dimension (spherical symmetry), β_{fix} is the fixed buffering capacity, D_{NH4+} and D_{Ac} are the ammonium and acetate diffusion coefficients (1270 and 700 μm²/s) and D_{NH3} and D_{HAc} are the restricted ammonia and acetic acid diffusion coefficients [29]. To simulate exposure to weak acid/base, the boundary condition (at r equal to nucleus radius) was set to represent the equilibrium composition of acetate or ammonium containing solution. Best-fitting to data yielded a β of 0.3 mM/pH and uncharged species diffusivity that was 3.7 orders of magnitude lower than the conjugate ion (Fig. 5Biii). Since 0.5 mM Hepes contributes ~0.2 mM/pH buffering at pH 6.9, fixed buffering in nuclei is inferred to be very weak.

3.5. Protons diffuse faster in the nucleus than in cytoplasm

The observations so far demonstrate that mobile buffers enter nuclei freely across nuclear pores (Fig. 4) and that fixed buffering capacity residing in the nucleus is very low (Fig. 5). Applying this information to Eq. (1) predicts that protons should diffuse faster in nucleoplasm than in cytoplasm (that is, the mobile fraction of buffering is higher in the nucleus). This prediction was tested experimentally in adult ventricular myocytes superfused with CO_2/HCO_3^--buffered Tyrode containing 0.5 mM 6-nitroveratraldehyde, a highly membrane-permeant, photolabile H^+-donor. By restricting the acid-uncaging site (*i.e.* 405 nm light exposure) to a small region of the cell and iterating between localized uncaging and whole-cell pH-image acquisition, it is possible to experimentally produce a point-source of acid and measure its dissipation throughout the cell [18]. Since high spatial resolution is required for measuring proton diffusion, Hoechst 33342 could not be used because the higher-intensity 405 nm laser needed for adequate spatial mapping of the nucleus would concurrently uncage acid from NVA. Thus, cSNARF1 fluorescence was used to measure diffusivity in cytoplasmic and nuclear regions. Myocytes were AM-loaded with cSNARF1 and fluorescence was recorded ratiometrically in linescan mode to improve temporal resolution. Between line-scanning for cSNARF1 (555 nm excitation), a high-intensity laser (405 nm) uncaged protons in a small segment of the linescan (Fig. 6A). This protocol had a temporal resolution (5.3 ms) sufficient to resolve diffusion delays over the small dimensions of cardiac nuclei (20 μm or less in long axis). To measure proton diffusivity in nucleoplasm, linescans were positioned to run along the long-axis of nuclear regions (Fig. 6Ai). In separate experiments, cytoplasmic diffusivity was determined from linescans that omit nuclear regions (Fig. 6Aii). The effective proton diffusion coefficient (D_H^{eff}) is inversely related to the time-delay between the proximal and distal $[H^+]$ time course (Fig. 6A). To quantify D_H^{eff}, $[H^+]$ time courses in two regions of interest along the linescan were best-fitted to simulations generated by a one-dimensional diffusion model [18]. The model solved the diffusion problem over the entire myocyte-length with reflection boundary conditions, and with a constant point-source of acid (F) positioned at the uncaging site:

$$\frac{d[H^+]}{dt} = D_H^{eff} \times \frac{\partial^2[H^+]}{\partial x^2} + F(x).$$

Results demonstrate that protons diffuse twice as fast in nucleoplasm compared to bulk cytoplasm (Fig. 6B), in agreement with the prediction of Eq. (1).

3.6. Nuclear Ca^{2+} dynamics can regulate the pH gradient between nucleus and cytoplasm

Inositol 1,4,5-trisphosphate ($InsP_3$), acting on $InsP_3$ receptors, regulates gene expression by triggering Ca^{2+} release from the nuclear envelope (NE), a structure that is continuous with the sarcoplasmic reticulum (SR) [12–14]. In the cytoplasm, $[Ca^{2+}]$ and pH are coupled *via* chemical interactions, such as binding to common buffers [9]. However, the relationship between nuclear $[Ca^{2+}]$ and pH_{nuc} is unknown. This was explored in adult ventricular myocytes dually loaded with cSNARF1 and Hoechst 33342. Myocytes, superfused in CO_2/HCO_3^--buffered Tyrode, were paced (1 Hz) to load the SR/NE with Ca^{2+}. Following a 3 minute resting period, pH_{nuc} was only marginally more alkaline than cytoplasm ($\Delta pH = pH_{nuc}\text{-}pH_{cyto} = 0.0324 \pm 0.0163$). Treatment with the $InsP_3$ receptor antagonist 2-aminoethoxydiphenyl borate (2-APB; 5 μM) made the nucleus more alkaline relative to the cytoplasm (Fig. 7A). Even after 20 min of treatment with 2-APB, pH_{nuc} was stably alkaline-shifted relative to pH_{cyto} ($\Delta pH = 0.092 \pm 0.017$; Fig. 7B). Emptying the SR/NE Ca^{2+} store with the SERCA inhibitor thapsigargin (10 μM; pre-treatment for 10 min) did not mimic the effect of 2-APB on pH_{nuc}, but collapsed ΔpH (Fig. 7B). Blocking SERCA is expected to raise nucleoplasm $[Ca^{2+}]$ as NE/SR stores become depleted. In contrast, 2-APB lowers nucleoplasm $[Ca^{2+}]$ by curtailing the leak [30]. Thus, pH_{nuc} in adult myocytes is influenced by Ca^{2+} signaling, producing the highest pH_{nuc} when nuclear $[Ca^{2+}]$ is low. Under physiological conditions, resting levels of Ca^{2+} signaling in the fully differentiated adult myocyte produce modestly alkaline nuclei. In contrast, nuclei of neonatal myocytes were more acidic than the surrounding cytoplasm ($\Delta pH = -0.041 \pm 0.012$). ΔpH in neonatal and adult myocytes were collapsed by the K^+/H^+ ionophore nigericin (10 μM) applied in high-K^+ superfusates (Fig. 2).

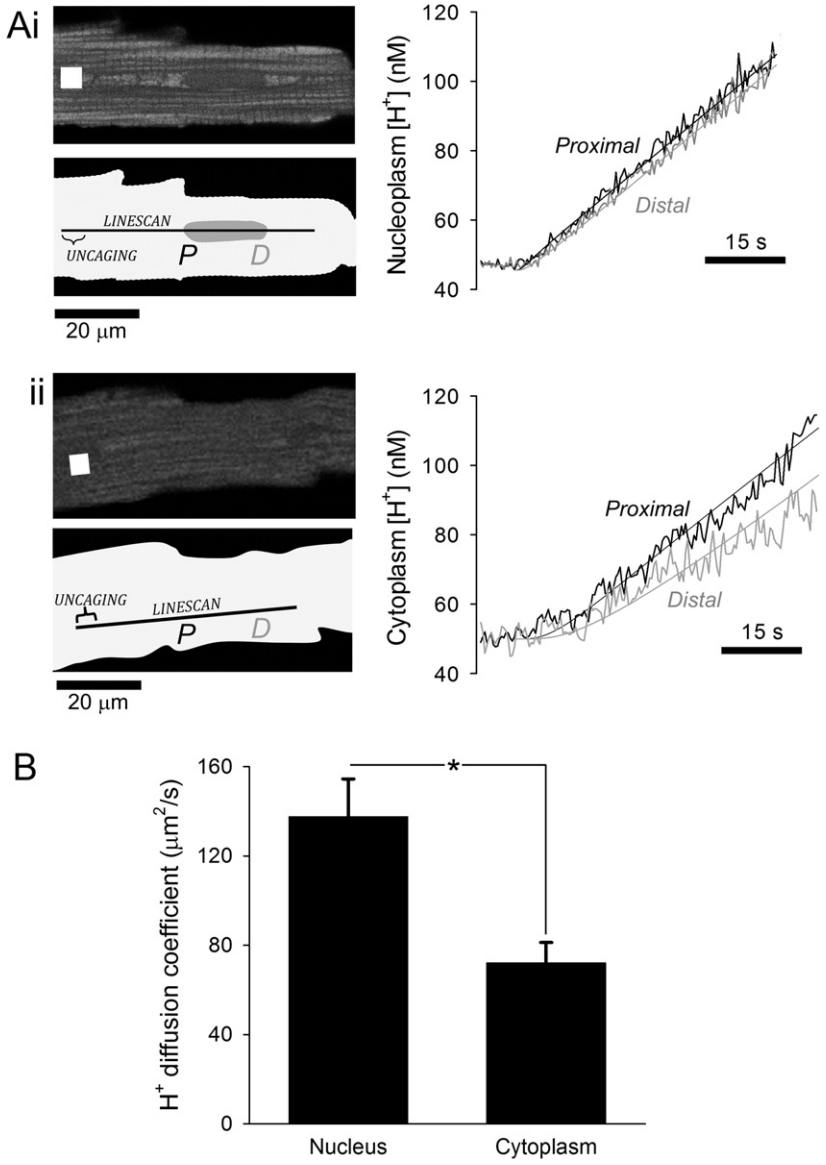

Fig. 6. Measuring proton diffusion coefficient in the adult myocyte nucleus. (A) cSNARF1-loaded myocyte. (i) Proton diffusivity measured along linescan through nuclear region (pinhole 2 μm). White region represents area of photolytic uncaging of acid from membrane permeant donor 6-nitroveratraldehyde (0.5 mM), supplied from superfusate. Uncaging alternated with linescaning for cSNARF1. Delay in $[H^+]$-rise measured at the proximal (nearest to the uncaging site, labeled *P*) and distal end (labeled *D*) of nucleus yields best-fit diffusion coefficient. Smooth lines show best-fit model simulation to data. (ii) Proton diffusivity measured along linescan that by-passes nuclear regions. (B) Proton diffusivity in the nucleus was twice as fast as in the cytoplasm ($n = 17, 11$; $P = 0.002$).

4. Discussion

This study explored proton dynamics in nuclei using a combination of fluorescence imaging and mathematical modeling. Biophysical characterization of the behavior of protons in the nucleus is necessary for understanding the regulation of pH_{nuc}. This information is relevant to nuclear biology because nucleic acids and nuclear proteins react with protons. To the best of our knowledge, this is the first study to simultaneously measure the pH in the nucleus and its surrounding cytoplasm in wild-type cardiac myocytes using non-protein fluorescent probes loaded passively into cells. This was achieved using two spectrally resolvable dyes, Hoechst 33342 and cSNARF1, which emit pH-sensitive (but Ca^{2+}-insensitive) fluorescence that can be quantified ratiometrically. Unlike pH-sensing proteins expressed in the nucleus [31], Hoechst dyes intercalate with DNA and probe pH in the DNA nano-environment, which is the domain relevant for regulating gene expression. The relevance of signal compartmentalization is emphasized by the ability of nuclear sensors to distinguish between Ca^{2+} evoked by $InsP_3$ signaling and 'contraction' Ca^{2+} evoked electrically [15]. Dual emission ratiometry eliminates motion artifacts and allows for accurate calibration in units of pH. Since measurements of nuclear and cytoplasmic pH can be performed on the same cell, the power to resolve pH gradients is high.

Proton dynamics in the cytoplasm are greatly influenced by the exceptionally high buffering capacity. In cardiac myocytes, the large (~mM/min) proton fluxes driven by the high turnover of ATP per cardiac cycle do not substantially affect cytoplasmic pH. As shown in Fig. 1, bulk cytoplasmic $[H^+]$ fluctuates by no more than 5% during a single cardiac cycle of an adult myocyte, in contrast to the dramatic changes in membrane potential, $[Ca^{2+}]$ and energetics. All parts of the myocyte that are adequately coupled by diffusion with the bulk cytoplasm are expected to have access to this buffering capacity. It is generally accepted that small ions can enter and exit the nucleus freely across large nuclear pores. Indeed, our data show that calcein, a medium-sized molecule similar in mass to ATP, diffuses into the nucleus as rapidly as it

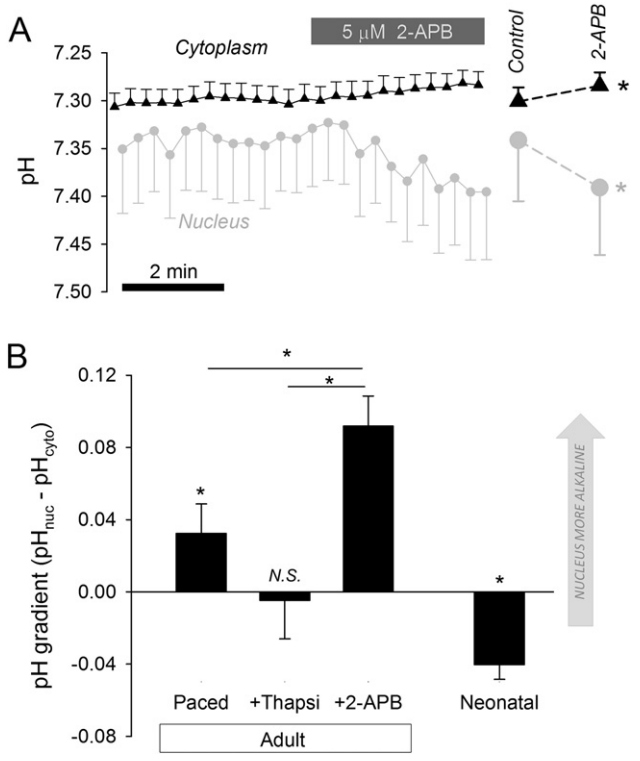

Fig. 7. Interactions between nuclear pH and nuclear Ca^{2+} signaling. (A) Adult ventricular myocytes dually loaded with cSNARF1 and Hoechst 33342 to measure cytoplasmic and nuclear pH simultaneously. 2-aminoethoxydiphenyl borate (2-APB; 5 μM) alkalinized the nucleus, resulting in a greater (more positive) nucleus-to-cytoplasm pH gradient ($P = 0.0072$ for nuclear response; $P = 0.0125$ for cytoplasmic response). (B) pH gradient in adult and neonatal ventricular myocytes measured at the steady-state attained after 20 min of treatment with 2-APB or thapsigargin (Thapsi; 10 μM). 2-APB produced stable nuclear alkalinization; Thapsi collapsed gradient. Relative to cytoplasm, neonatal myocyte nuclei were significantly acidic ($P < 10^{-7}$).

does in bulk cytoplasm of neonatal and adult cardiac myocytes (Fig. 3). Emptying the SR/NE Ca^{2+} store did not affect calcein mobility, arguing that the permeability of pores to medium-sized molecules is independent of NE $[Ca^{2+}]$. These observations suggest that nuclear pores and the nucleoplasm collectively exert the same resistance to diffusion as the cytoplasm.

In light of the observation that nuclear pores do not substantially restrict calcein diffusion, it was surprising to find that proton transmission in and out of the nucleus can be relatively slow. Protons were only able to access the nucleoplasm if sufficient mobile buffering was available (Fig. 4A, D). This inference is consistent with the unique properties of protons, largely because of their high reactivity. As illustrated mathematically by Eq. (1), free diffusion of protons is made negligible by high buffering capacity; instead, effective proton mobility is described exclusively by the properties of buffers. Because of their large lumen, nuclear pores cannot support special forms of proton diffusion (*e.g.* Grotthuss [32]) that normally take place across proton channels. Our data suggest that the exchange of protons between nucleus and cytoplasm takes place by means of facilitated diffusion aboard mobile buffers. These act as proton carriers that shuttle between the nucleus and cytoplasm down concentration gradients. Experimentally, mobile buffers were delivered to permeabilized cells from the superfusate. In intact cells, mobile buffering is provided by intrinsic molecules supplied by cytoplasm (such as phosphates, amino acids and dipeptides) plus the extrinsic buffer CO_2/HCO_3^-. Collectively, intrinsic mobile buffers account for ~10 mM/pH buffering capacity in cardiac myocyte cytoplasm [17]. The effectiveness of CO_2/HCO_3^- to act as a mobile buffer is limited by its slow spontaneous reaction kinetics that could be accelerated by carbonic anhydrase (CA) activity [20]. To date, none of the mammalian CA isoforms are known to target to the nucleus [33], thus CO_2/HCO_3^- may be relatively ineffective as a mobile carrier of nuclear protons. Thus, considering the normal range of myocyte mobile buffering, protons are transmitted in and out of the nucleus no faster than calcein, despite being 600-fold smaller (Fig. 4D).

Fixed pH buffers resident in the nucleus cannot facilitate proton transport, but will influence the magnitude and rate of pH_{nuc} changes. Surprisingly, our data (Fig. 5) suggest that fixed buffering (β_{fix}) in the nucleus is very weak. This was inferred from the amplitude of pH_{nuc} transients evoked by photolytic acid uncaging in permeabilized adult myocytes and exposure of permeabilized HCT116 to weak acids or bases. Low β_{fix} (~1 mM/pH) is somewhat surprising, given the presence of protonatable sites on nucleic acids and nuclear proteins. However, half of the nuclear mass is DNA which is only a weak buffer at resting pH because the pK_a of its bases and phosphate backbone is outside the physiological pH range. A consequence of low nuclear β_{fix} is at least three-fold. Firstly, the nucleus is reliant on other parts of the cell to supply buffers for protecting the genome against pH disturbances. Secondly, the nucleus is more prone to developing out-of-equilibrium pH transients during evoked proton fluxes. Thirdly, effective proton diffusivity (D_H^{eff}) in the nucleus is predicted to be faster than in bulk cytoplasm. In myocyte cytoplasm at resting pH_i, a third of total buffering capacity is due to CO_2/HCO_3^- [18]. Of the remainder, a third is attributable to intrinsic mobile buffers. Therefore, 40–50% of total buffering in cytoplasm arises from fixed moieties. Assuming D_{mob} and β_{mob} are no different between nucleus and cytoplasm, Eq. (1) predicts a doubling of diffusivity in the nucleus. Indeed, D_H^{eff} in the nucleus was found to be twice its cytoplasmic value (Fig. 6).

The nucleus hosts a specialized Ca^{2+} signaling apparatus that is implicated in the control of gene expression. Our data show that altering nuclear Ca^{2+} signaling also affects pH_{nuc}. Blocking $InsP_3$ receptor channels (with 2-APB) was found to selectively alkalize pH_{nuc}, thereby increasing the magnitude of the pH gradient across the nuclear envelope (ΔpH) (Fig. 7). Intriguingly, the change in ΔpH was stable which indicates that an uphill transport mechanism must balance dissipative proton backflux. Previous studies have measured nuclear pH to be higher than cytoplasm [28]. This apparent ΔpH gradient may arise from a trans-NE potential (V_{NE}), Gibbs–Donnan forces, differences in ionization, or an artifact of dye calibration [21]. Our finding that ΔpH can change dynamically with maneuvers that affect Ca^{2+} signaling argues against dye artifacts. Moreover, addition of nigericin (K^+/H^+) abolished pH gradients (Fig. 2). Previous electrophysiological measurements have shown that the nucleus is negatively charged relative to the cytoplasm (V_{NE} in the range −10 to −5 mV [21]), which would *per se* result in a negative ΔpH of ~−0.1 units at equilibrium (acidic nucleus). Instantaneously blocking Ca^{2+} release *via* $InsP_3$ receptors at the inner nuclear membrane could be expected to make the nucleus more negatively charged, *i.e.* more acidic. This prediction goes against our experimental observations. The excess of anionic charge in the nucleus has been suggested to generate a Gibbs–Donnan equilibrium favoring nuclear acidity. Blocking Ca^{2+} release may reduce the extent to which anionic charge is neutralized by Ca^{2+}, thereby exacerbating the Gibbs–Donnan effect. Again, this prediction contradicts our findings. The nucleoplasm is more hydrophobic than the cytoplasm, and hence has a lower dielectric constant. *In vitro*, this tends to decrease weak acid ionization [28] and would predict an alkaline pH_{nuc} (Fig. 8A), as observed at the steady-state (Fig. 7). However, this model, alone, is inadequate because it cannot explain how abrupt inhibition of Ca^{2+} signaling could evoke a change in ΔpH. The underlying mechanism must account for the observation that increasing NE Ca^{2+} load (thapsigargin < paced cells < 2-APB) correlates with pH_{nuc} (Fig. 7B).

The circuit for Ca^{2+} signaling in the myocyte nucleus is proposed to involve release at the inner nuclear membrane (*via* $InsP_3$ receptors) and uptake at the outer nuclear membrane (*via* SERCA pumps). As shown experimentally by others [30], blocking release would lower $[Ca^{2+}]_{nuc}$ (Fig. 8B). In contrast, inhibiting SERCA activity would raise $[Ca^{2+}]_{nuc}$

(Fig. 8C). Normal Ca^{2+} signaling is expected to produce intermediate $[Ca^{2+}]_{nuc}$. Raising $[Ca^{2+}]_{nuc}$ may acidify the nucleus by displacing protons from buffering moieties that also bind Ca^{2+} ions. Such a competitive interaction is known to occur in cytoplasm and is mediated, at least in part, by histidyl dipeptides [9] which are predicted to be a major contributor to nuclear pH buffering. However, diffusive coupling (albeit slow) between the nucleus and cytoplasm would eventually dissipate pH gradients. Thus, an uphill form of proton transport is required to stabilize ΔpH.

The recently described cytoplasmic Ca^{2+}/H^+ exchanger [9] may provide a mechanism for stabilizing pH gradients across the NE. According to this model, a mobile buffer that binds Ca^{2+} ions and protons competitively can produce Ca^{2+} transport up a $[H^+]$ gradient, or *vice versa*. To explore how this may apply to the nucleus, we first consider Ca^{2+} cycling across the NE. In order to couple $InsP_3$ receptor release with SERCA uptake, Ca^{2+} ions must diffuse *via* nuclear pores. The nuclear pore density is 10–40 per μm^2 [21] and assuming that this is distributed evenly, the longest $InsP_3$ receptor-to-SERCA path-length can be 35–130 nm, *i.e.* a distance that precludes free Ca^{2+} ion diffusion and implies a role for Ca^{2+} buffers in completing the circuit [34]. SR Ca^{2+} release in diastole is 0.3 μM/s [35] and increases substantially during electrical stimulation. If a comparable flux of Ca^{2+} is released into the nucleoplasm, it would drive a major efflux of Ca^{2+}-bound buffers from the nucleus. The continuous efflux of Ca^{2+}-bound buffer provides an opportunity for uphill transport of cargo aboard the returning (Ca^{2+}-free) buffer. The Ca^{2+}-free buffer is expected to be more anionic and have higher proton affinity (K_a). If this were in the physiological pH range, the returning buffer molecules would carry a significant proton cargo to acidify the nucleus. Since protons can only enter the nucleus aboard mobile buffers, dissipative back-flux would be readily surmountable. The modeling framework presented in [9] can be used to predict the conditions that favor a large trans-NE $[H^+]$ gradient relative to the $[Ca^{2+}]$ gradient ($\Delta[H^+]/\Delta[Ca^{2+}]$). A high $\Delta[H^+]/\Delta[Ca^{2+}]$ ratio would be attained by a combination of high Ca^{2+} affinity of mobile buffers, high nuclear Ca^{2+} buffering relative to cytoplasm, and low β_{fix}. Thus, the low nuclear β_{fix} measured experimentally (Fig. 5) would support the development of ΔpH during Ca^{2+} signals. The inversion of ΔpH from positive (alkaline nucleus) in adults to negative (acidic nucleus) in neonates may relate to different degrees of nuclear Ca^{2+} signaling engaged at different stages of development and differentiation.

5. Conclusions

Despite the presence of high-conductance nuclear pores, protons can only enter (or exit) the nucleus when bound to mobile buffers. This carrier-mediated transport results in surprisingly slow proton transmission. Mobile buffers, ultimately supplied by the cytoplasm, account for the majority of nuclear pH buffering because of the low concentration of fixed buffering moieties in nucleoplasm. As a result of this unique buffering milieu, protons in the nucleus diffuse faster than in the cytoplasm. Nuclear Ca^{2+} signals can evoke changes in nuclear pH, and generate stable pH gradients, possibly maintained as a result of a Ca^{2+}/H^+ exchange process involving mobile buffers that bind Ca^{2+} ions and protons competitively. Nuclear biology is strongly regulated by Ca^{2+} signaling, but the importance of pH_{nuc} as an intermediary of this cascade or as a *bona fide* signal merits further investigation.

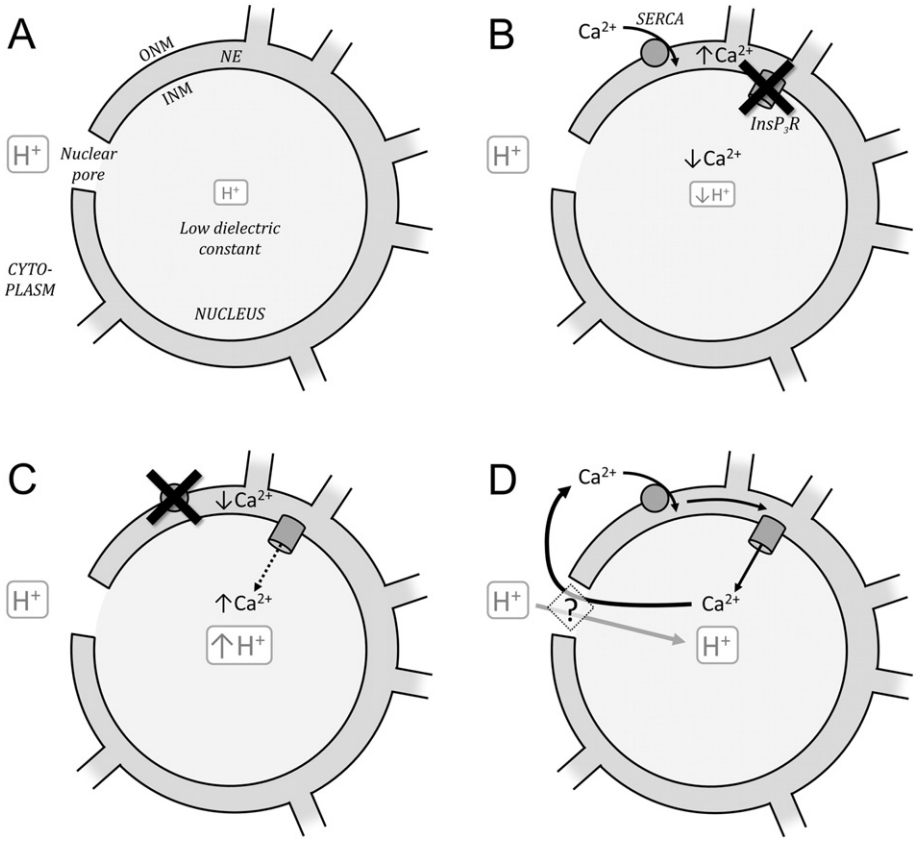

Fig. 8. Nuclear pH-Ca^{2+} interactions. Hypothesis. (A) Nucleoplasm hydrophobicity (low dielectric constant) reduces ionization of protonated sites, resulting in alkaline nuclear pH relative to cytoplasm. NE—nuclear envelope; ONM—outer nuclear membrane; INM—inner nuclear membrane. (B) Loading the NE with Ca^{2+} by SERCA pumps at the ONM, in the absence of Ca^{2+} leak across $InsP_3$ receptors ($InsP_3R$) on the INM, results in low nucleoplasmic $[Ca^{2+}]$. This maintains an alkaline pH_{nuc}. (C) Inhibition of SERCA allows nuclear $[Ca^{2+}]$ to rise. This acidifies the nucleus, possibly by displacing protons from Ca^{2+}-binding sites. (D) During normal signaling, Ca^{2+} released from the NE *via* open $InsP_3R$ is recycled back to the NE by SERCA. Since these processes operate at opposite sides of the NE, they must be coupled by Ca^{2+} diffusion across nuclear pores. This process may maintain nuclear pH at a more acidic level by exchanging Ca^{2+}-bound mobile buffers with protonated mobile buffers.

Disclosures

None declared.

Acknowledgments

We thank Professor Richard Vaughan-Jones for valuable comments and mentoring throughout the project. We thank Dr. Mark Richards for isolating adult cardiac myocytes and Drs. Alexander Burdyga and Stefania Monterisi for culturing neonatal cardiac myocytes. Supported by the British Heart Foundation (PG/12/2/29324) and the EP Abraham Fund (CF 255). P.S. is a Royal Society University Research Fellow.

References

[1] R.D. Vaughan-Jones, K.W. Spitzer, P. Swietach, Intracellular pH regulation in heart, J. Mol. Cell. Cardiol. 46 (2009) 318–331.
[2] E.J. Crampin, N.P. Smith, A.E. Langham, R.H. Clayton, C.H. Orchard, Acidosis in models of cardiac ventricular myocytes, Philos. Transact. A Math. Phys. Eng. Sci. 364 (2006) 1171–1186.
[3] L. Chen, J.N. Glover, P.G. Hogan, A. Rao, S.C. Harrison, Structure of the DNA-binding domains from NFAT, Fos and Jun bound specifically to DNA, Nature 392 (1998) 42–48.
[4] D.C. Mikles, V. Bhat, B.J. Schuchardt, B.J. Deegan, K.L. Seldeen, C.B. McDonald, et al., pH modulates the binding of early growth response protein 1 transcription factor to DNA, FEBS J. 280 (2013) 3669–3684.
[5] B.J. Deegan, K.L. Seldeen, C.B. McDonald, V. Bhat, A. Farooq, Binding of the ERalpha nuclear receptor to DNA is coupled to proton uptake, Biochemistry 49 (2010) 5978–5988.
[6] T. Lundback, S. van Den Berg, T. Hard, Sequence-specific DNA binding by the glucocorticoid receptor DNA-binding domain is linked to a salt-dependent histidine protonation, Biochemistry 39 (2000) 8909–8916.
[7] P.H. Sugden, Signaling in myocardial hypertrophy: life after calcineurin? Circ. Res. 84 (1999) 633–646.
[8] J.H. van Berlo, M. Maillet, J.D. Molkentin, Signaling effectors underlying pathologic growth and remodeling of the heart, J. Clin. Invest. 123 (2013) 37–45.
[9] P. Swietach, J.B. Youm, N. Saegusa, C.H. Leem, K.W. Spitzer, R.D. Vaughan-Jones, Coupled Ca^{2+}/H^{+} transport by cytoplasmic buffers regulates local Ca^{2+} and H^{+} ion signaling, Proc. Natl. Acad. Sci. U. S. A. 110 (2013) E2064–E2073.
[10] P. Swietach, K.W. Spitzer, R.D. Vaughan-Jones, Na(+) ions as spatial intracellular messengers for co-ordinating Ca(2)(+) signals during pH heterogeneity in cardiomyocytes, Cardiovasc. Res. 105 (2015) 171–181.
[11] H.S. Choi, A.W. Trafford, C.H. Orchard, D.A. Eisner, The effect of acidosis on systolic Ca^{2+} and sarcoplasmic reticulum calcium content in isolated rat ventricular myocytes, J. Physiol. 529 (Pt 3) (2000) 661–668.
[12] X. Wu, T. Zhang, J. Bossuyt, X. Li, T.A. McKinsey, J.R. Dedman, et al., Local InsP3-dependent perinuclear Ca^{2+} signaling in cardiac myocyte excitation–transcription coupling, J. Clin. Invest. 116 (2006) 675–682.
[13] D.R. Higazi, C.J. Fearnley, F.M. Drawnel, A. Talasila, E.M. Corps, O. Ritter, et al., Endothelin-1-stimulated InsP3-induced Ca^{2+} release is a nexus for hypertrophic signaling in cardiac myocytes, Mol. Cell 33 (2009) 472–482.
[14] F. Hohendanner, A.D. McCulloch, L.A. Blatter, A.P. Michailova, Calcium and IP_3 dynamics in cardiac myocytes: experimental and computational perspectives and approaches, Front. Pharmacol. 5 (2014) 35.
[15] S. Ljubojevic, D.M. Bers, Nuclear calcium in cardiac myocytes, J. Cardiovasc. Pharmacol. 65 (2015) 211–217.
[16] C.D. Garciarena, J.B. Youm, P. Swietach, R.D. Vaughan-Jones, H(+)-activated Na(+) influx in the ventricular myocyte couples Ca(2)(+)-signalling to intracellular pH, J. Mol. Cell. Cardiol. 61 (2013) 51–59.
[17] R.D. Vaughan-Jones, B.E. Peercy, J.P. Keener, K.W. Spitzer, Intrinsic H(+) ion mobility in the rabbit ventricular myocyte, J. Physiol. 541 (2002) 139–158.
[18] P. Swietach, K.W. Spitzer, R.D. Vaughan-Jones, pH-dependence of extrinsic and intrinsic H(+)-ion mobility in the rat ventricular myocyte, investigated using flash photolysis of a caged-H(+) compound, Biophys. J. 92 (2007) 641–653.
[19] C.H. Leem, D. Lagadic-Gossmann, R.D. Vaughan-Jones, Characterization of intracellular pH regulation in the guinea-pig ventricular myocyte, J. Physiol. 517 (Pt 1) (1999) 159–180.
[20] C.H. Leem, R.D. Vaughan-Jones, Out-of-equilibrium pH transients in the guinea-pig ventricular myocyte, J. Physiol. 509 (Pt 2) (1998) 471–485.
[21] M. Mazzanti, J.O. Bustamante, H. Oberleithner, Electrical dimension of the nuclear envelope, Physiol. Rev. 81 (2001) 1–19.
[22] R.S. Balaban, Perspectives on: SGP symposium on mitochondrial physiology and medicine: metabolic homeostasis of the heart, J Gen. Physiol. 139 (2012) 407–414.
[23] M.J. Kushmerick, Multiple equilibria of cations with metabolites in muscle bioenergetics, Am. J. Physiol. 272 (1997) C1739–C1747.
[24] H. Gorner, Direct and sensitized photoprocesses of bis-benzimidazole dyes and the effects of surfactants and DNA, Photochem. Photobiol. 73 (2001) 339–348.
[25] J.A. Thomas, R.N. Buchsbaum, A. Zimniak, E. Racker, Intracellular pH measurements in Ehrlich ascites tumor cells utilizing spectroscopic probes generated in situ, Biochemistry 18 (1979) 2210–2218.
[26] M. Irving, J. Maylie, N.L. Sizto, W.K. Chandler, Intracellular diffusion in the presence of mobile buffers. Application to proton movement in muscle, Biophys. J. 57 (1990) 717–721.
[27] M.A. Schroeder, M.A. Ali, A. Hulikova, C.T. Supuran, K. Clarke, R.D. Vaughan-Jones, et al., Extramitochondrial domain rich in carbonic anhydrase activity improves myocardial energetics, Proc. Natl. Acad. Sci. U. S. A. 110 (2013) E958–E967.
[28] O. Seksek, J. Bolard, Nuclear pH gradient in mammalian cells revealed by laser microspectrofluorimetry, J. Cell Sci. 109 (Pt 1) (1996) 257–262.
[29] P. Swietach, C.H. Leem, K.W. Spitzer, R.D. Vaughan-Jones, Experimental generation and computational modeling of intracellular pH gradients in cardiac myocytes, Biophys. J. 88 (2005) 3018–3037.
[30] S. Ljubojevic, S. Walther, M. Asgarzoei, S. Sedej, B. Pieske, J. Kockskamper, In situ calibration of nucleoplasmic versus cytoplasmic Ca^{2+} concentration in adult cardiomyocytes, Biophys. J. 100 (2011) 2356–2366.
[31] J. Llopis, J.M. McCaffery, A. Miyawaki, M.G. Farquhar, R.Y. Tsien, Measurement of cytosolic, mitochondrial, and Golgi pH in single living cells with green fluorescent proteins, Proc. Natl. Acad. Sci. U. S. A. 95 (1998) 6803–6808.
[32] S. Cukierman, Et tu, Grotthuss! and other unfinished stories, Biochim. Biophys. Acta 1757 (2006) 876–885.
[33] C.T. Supuran, Carbonic anhydrases: novel therapeutic applications for inhibitors and activators, Nat. Rev. Drug Discov. 7 (2008) 168–181.
[34] E. Neher, Usefulness and limitations of linear approximations to the understanding of Ca^{++} signals, Cell Calcium 24 (1998) 345–357.
[35] R.A. Bassani, D.M. Bers, Rate of diastolic Ca release from the sarcoplasmic reticulum of intact rabbit and rat ventricular myocytes, Biophys. J. 68 (1995) 2015–2022.